

# Pseudo Block Coded Single-Carrier Transmission Using Frequency-Domain Block Signal Detection

Hiroyuki MIYAZAKI<sup>†</sup> and Fumiyuki ADACHI<sup>‡</sup>

Dept. of Communications Engineering, Graduate School of Engineering, Tohoku University  
6-6-05 Aza-Aoba, Aramaki, Aoba-ku, Sendai, 980-8579 Japan

<sup>†</sup>miyazaki@mobile.ecei.tohoku.ac.jp, <sup>‡</sup>adachi@ecei.tohoku.ac.jp

**Abstract**— Recently, we proposed a pseudo block coded single-carrier (PBC-SC) transmission using minimum mean square error (MMSE) based frequency-domain equalization and decoding (FDED) and show that MMSE based FDED achieves BER performance superior to 2-step decoding (which performs frequency-domain equalization and hard decision decoding separately). However, there still exists a large BER performance gap between MMSE based FDED and MF bound due to the presence of residual inter-symbol interference (ISI) after MMSE based FDED. In this paper, in order to narrow the performance gap, we propose frequency-domain block signal detection (FDBD) aided FDEs for PBC-SC transmission: frequency-domain iterative interference cancellation (FDIC), maximum likelihood block signal detection employing QR decomposition and M algorithm (QRM-MLBD) and belief propagation (BP). We compare, by computer simulation, the BER performances and the computational complexities of three FDBD aided FDED schemes. It is shown that QRM-MLBD and BP can achieve almost the same BER performance as MF bound with much lower computational complexity than MMSE based FDED.

**Keywords**— component; Frequency-domain equalization, frequency-domain block signal detection, single-carrier transmission

## I. INTRODUCTION

Bit error rate (BER) performance of broadband single-carrier (SC) transmission significantly degrades due to inter-symbol interference (ISI) caused by frequency-selective fading [1]. Minimum mean square error (MMSE) based frequency-domain equalization (FDE) can take advantage of channel frequency-selectivity to improve the transmission performance [2-4].

In wireless communications, channel coding is necessary to improve the BER performance [1]. Block coding and hard-decision decoding has low computational complexity, but its error correction ability is low. Maximum likelihood (ML) decoding has high error correction ability, however, its computational complexity is very high.

Recently, we proposed a pseudo block coded (PBC)-SC transmission using minimum mean square error (MMSE) based frequency-domain equalization and decoding (FDED) [5]. In PBC-SC transmission using FDED, FDE and pseudo block decoding are jointly performed. We showed that MMSE based FDED provides the BER performance superior to 2-step decoding (which performs FDE and hard decision decoding separately). However, there still exists a large BER performance gap between MMSE based FDED and MF bound due to the presence of residual ISI after MMSE based FDED. In this paper, we will deal with narrowing the performance gap.

In PBC-SC transmission, a concatenation of channel matrix, mapping matrix, DFT matrix, interleaving matrix and

pseudo block encoding matrix can be viewed as an equivalent MIMO channel. Therefore, frequency-domain block signal detection (FDBD) [6-9] can be applied to PBC-SC transmission as a new FDED scheme. Furthermore, since the equivalent MIMO channel of PBC-SC transmission is a massive MIMO channel, low complexity detection based on belief propagation (BP) for a massive MIMO system proposed in [10,11] can be also applied to PBC-SC transmission.

In this paper, we propose FDBD aided FDED for PBC-SC transmission in order to narrow the performance gap from MF bound. In the proposed scheme, FDE and pseudo block decoding are jointly performed by FDBD to further suppress the residual ISI compared to MMSE based FDED. We present three FDBD aided FDED schemes: frequency-domain iterative interference cancellation (FDIC) [6,7], maximum likelihood block signal detection employing QR decomposition and M algorithm (QRM-MLBD) [8,9] and BP [10,11]. It is shown by computer simulation that PBC-SC transmission can reduce the number of surviving paths for M algorithm and as a consequence, QRM-MLBD requires lower complexity than MMSE based FDED while achieving almost the same BER performance as MF bound. Also shown is that BP also achieves BER performance similar to MF bound with about 8 times lower computational complexity compared to MMSE based FDED.

The remainder of this paper is organized as follows. Sect. II presents PBC-SC transmission and Sect. III describes three FDBD aided FDED schemes. Computer simulation results are presented and discussed in Sect. IV. Sect. V offers conclusion.

## II. PSEUDO BLOCK CODED SC TRANSMISSION

In this paper, we consider PBC-SC transmission [5]. We assume that the transmitter and receiver equip with single antenna, respectively. The transmitter and receiver structures in PBC-SC transmission are illustrated in Fig. 1. At the transmitter, the pseudo block coded sequence, which consists of  $k$  symbols, are generated by applying  $(k,n)$  pseudo block coding to a sequence of  $n$  data modulated symbols. After generating  $N_{code}$  pseudo block coded sequences, interleaving is performed. The sequence of  $kN_{code}$  pseudo block coded symbols after interleaving is transformed into the frequency-domain signal by  $kN_{code}$ -point discrete Fourier transform (DFT) and then mapped to  $N_c$  subcarriers. The frequency-domain signal after mapping is transformed back to the time-domain signal by  $N_c$ -point inverse fast Fourier transform (IFFT). After inserting the cyclic prefix (CP) into the beginning of the transmit signal block, the transmitter transmits it to the receiver.

At the receiver, after CP removal, the received signal is transformed into the frequency-domain signal by  $N_c$ -point FFT. Then, FDE, de-mapping, IDFT, de-interleaving and pseudo

block decoding are jointly performed by FDBD aided FDED and finally, data demodulation is carried out.

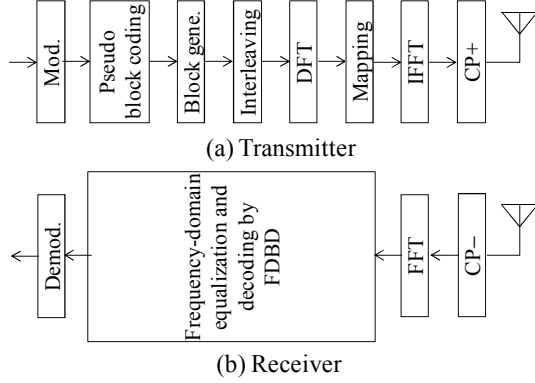


Fig. 1. Transmitter/receiver structures.

### A. Signal representation

Throughout this paper, the symbol-spaced discrete time representation is used.

At the transmitter,  $N_{code}$  pseudo block coded symbol sequences, which consist of  $k$  symbols, are generated by applying pseudo block encoding to the data modulated symbol sequences. The  $m$ th ( $m=0, \dots, N_{code}-1$ ) pseudo block coded symbol vector  $\mathbf{c}_m = [c_m(0), \dots, c_m(k-1)]^T$  is given as

$$\mathbf{c}_m = \mathbf{C}\mathbf{d}_m, \quad (1)$$

where  $\mathbf{d}_m = [d_m(0), \dots, d_m(n-1)]^T$  is the  $m$ th data modulated symbol vector and  $\mathbf{C}$  is  $k \times n$  pseudo block encoding matrix. After interleaving, the sequence of  $kN_{code}$  symbols is transformed into the frequency-domain transmit signal by  $kN_{code}$ -point DFT, and then, mapped to  $N_c$  subcarriers. The frequency-domain transmit signal after mapping is transformed back to the time-domain signal by  $N_c$ -point IFFT. After CP insertion, the coded signal is transmitted over a frequency-selective channel.

At the receiver, after CP removal, the received signal is transformed into the frequency-domain received signal by  $N_c$ -point FFT. The frequency-domain received signal vector  $\mathbf{Y} = [Y(0), \dots, Y(N_c-1)]^T$  can be expressed as

$$\mathbf{Y} = \sqrt{2P}\mathbf{H}\mathbf{M}\mathbf{F}\mathbf{B}\bar{\mathbf{C}}\bar{\mathbf{d}} + \mathbf{N}, \quad (2)$$

where  $P$  is the received signal power.  $\mathbf{H} = \text{diag}\{H(0), \dots, H(N_c-1)\}$  denotes  $N_c \times N_c$  channel matrix and  $H(j)$  is the  $j$ th frequency channel transfer function.  $\mathbf{F}$  is  $kN_{code} \times kN_{code}$  DFT matrix and given as

$$\mathbf{F} = \frac{1}{\sqrt{kN_{code}}} \begin{bmatrix} e^{-j\frac{2\pi \cdot 0 \cdot 0}{kN_{code}}} & e^{-j\frac{2\pi \cdot 0 \cdot 1}{kN_{code}}} & \dots & e^{-j\frac{2\pi \cdot 0 \cdot (kN_{code}-1)}{kN_{code}}} \\ e^{-j\frac{2\pi \cdot 1 \cdot 0}{kN_{code}}} & e^{-j\frac{2\pi \cdot 1 \cdot 1}{kN_{code}}} & \dots & \vdots \\ \vdots & \vdots & \ddots & \vdots \\ e^{-j\frac{2\pi \cdot (kN_{code}-1) \cdot 0}{kN_{code}}} & \dots & \dots & e^{-j\frac{2\pi \cdot (kN_{code}-1) \cdot (kN_{code}-1)}{kN_{code}}} \end{bmatrix}. \quad (3)$$

$\mathbf{M}$  denotes  $N_c \times kN_{code}$  mapping matrix and  $\mathbf{B}$  is  $kN_{code} \times kN_{code}$  interleaving matrix.  $\mathbf{C}$  and  $\bar{\mathbf{d}}$  are  $kN_{code} \times nN_{code}$  expanded pseudo block encoding matrix and expanded data modulated symbol vector, respectively. They are expressed as

$$\bar{\mathbf{C}} = \begin{bmatrix} \mathbf{C} & \mathbf{0} \\ & \ddots \\ \mathbf{0} & \mathbf{C} \end{bmatrix}, \quad \bar{\mathbf{d}} = \begin{bmatrix} \mathbf{d}_0 \\ \vdots \\ \mathbf{d}_{N_{code}-1} \end{bmatrix}. \quad (4)$$

$\mathbf{N} = [N(0), \dots, N(N_c-1)]^T$  is noise vector and  $N(j)$  denotes the zero-mean complex valued additive white Gaussian noise (AWGN) having variance  $2N_0/T_s$  with  $N_0$  and  $T_s$  being the single-sided power spectrum density of AWGN and the symbol duration, respectively.

(2) can be rewritten as

$$\mathbf{Y} = \sqrt{2P}\hat{\mathbf{H}}\bar{\mathbf{d}} + \mathbf{N}, \quad (5)$$

where  $\hat{\mathbf{H}} = \mathbf{H}\mathbf{M}\mathbf{F}\mathbf{B}\bar{\mathbf{C}}$  is  $N_c \times nN_{code}$  equivalent channel matrix. It is seen from (5) that the concatenation of the channel matrix, the mapping matrix, DFT matrix, the interleaving matrix and the expanded pseudo block encoding matrix can be viewed as an equivalent MIMO channel. Therefore, FDE, de-mapping, IDFT, de-interleaving and pseudo block decoding can be jointly performed by applying FDBD aided FDED.

### III. FDBD AIDED FDED

In this paper, we propose three FDBD aided FDED schemes: FDIC, QRM-MLBD and BP.

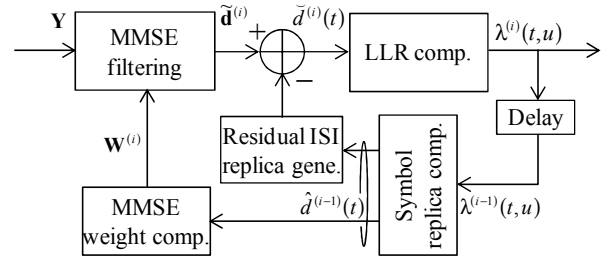


Fig. 2. Flowchart of FDIC.

### A. FDIC

Fig. 2 shows the flowchart of FDIC. FDIC consists of MMSE filtering, residual ISI cancellation, log-likelihood ratio (LLR) computation, symbol replica generation, ISI replica generation and MMSE weight computation. Above operations are repeated by  $I$  iterations and finally, data demodulation is performed.

Below, we focus on the  $i$ th ( $i=0, \dots, I-1$ ) iteration. At first, FDE, de-mapping, IDFT, de-interleaving, and pseudo block decoding are jointly performed by MMSE filtering. The received signal vector,  $\tilde{\mathbf{d}}^{(i)} = [\tilde{d}^{(i)}(0), \dots, \tilde{d}^{(i)}(nN_{code}-1)]^T$ , after MMSE filtering is given as

$$\tilde{\mathbf{d}}^{(i)} = \mathbf{W}^{(i)}\mathbf{Y}, \quad (6)$$

where  $\mathbf{W}^{(i)}$  is  $nN_{code} \times N_c$  MMSE filter in the  $i$ th iteration. MMSE filter is designed so as to minimize the mean square error (MSE) between the transmit signal before pseudo block encoding and the received signal after residual ISI cancellation and given as

$$\mathbf{W}^{(i)} = \hat{\mathbf{H}}^H (\hat{\mathbf{H}}\mathbf{G}^{(i)}\hat{\mathbf{H}}^H + \gamma\mathbf{I}_{N_c})^{-1}, \quad (7)$$

where  $\gamma$  is the received SNR and  $\mathbf{I}_N$  is  $N \times N$  identity matrix.  $\mathbf{G}^{(i)} = \text{diag}\{G^{(i)}(0), \dots, G^{(i)}(nN_{code}-1)\}$  is residual ISI factor and given as

$$G^{(i)}(t) = 1 - |\hat{d}^{(i-1)}(t)|^2 \quad \text{for QPSK}, \quad (8)$$

where  $\hat{d}^{(i-1)}(t)$  is soft-decision symbol replica generated in the  $(i-1)$ th iteration. The residual ISI cancellation is performed to the received signal after MMSE filtering. The  $i$ th received signal,  $\tilde{d}^{(i)}(t)$ , after the residual ISI cancellation is given as

$$\bar{d}^{(i)}(t) = \tilde{d}^{(i)}(t) - \sqrt{2P} \sum_{\substack{t'=0 \\ \neq t}}^{nN_{code}-1} (\mathbf{W}^{(i)}(t) \hat{\mathbf{H}}(t')) \hat{d}^{(i-1)}(t'), \quad (9)$$

where  $\mathbf{W}^{(i)}(t)$  is the  $t$ th row vector of MMSE filter and  $\hat{\mathbf{H}}(t')$  is the  $t'$ th column vector of the equivalent MIMO channel, respectively. After the residual ISI cancellation, LLR,  $\lambda^{(i)}(t,u)$ , of the  $u$ th bit in the  $t$ th symbol is computed. The soft-decision symbol replica is generated by using LLR and then, MMSE filter and the residual ISI replica are re-computed by using the soft-decision symbol replica given as (7) and (9). The above processes are repeated by  $I$  iterations and finally, data demodulation is carried out.

### B. QRM-MLBD

In QRM-MLBD, The equivalent MIMO channel matrix is transformed into an upper triangle matrix and hence, MLD has a tree structure. Therefore, the computational complexity can be reduced by applying M algorithm [8,9].

(5) can be rewritten as

$$\mathbf{Y} = \sqrt{2P} \mathbf{Q} \mathbf{R} \bar{\mathbf{d}} + \mathbf{N}, \quad (10)$$

where  $\mathbf{Q}$  is  $N_c \times nN_{code}$  matrix which satisfies  $\mathbf{Q}^H \mathbf{Q} = \mathbf{I}_{nN_{code}}$  and  $\mathbf{R}$  is  $nN_{code} \times nN_{code}$  upper triangle matrix. Therefore, by multiplying  $\mathbf{Q}^H$  to the frequency-domain received signal, the frequency-domain received signal can be transformed as

$$\mathbf{Z} = [Z(0, \dots, nN_{code} - 1)]^T = \mathbf{Q}^H \mathbf{Y} = \sqrt{2P} \mathbf{R} \bar{\mathbf{d}} + \mathbf{Q}^H \mathbf{N}$$

$$= \sqrt{2P} \begin{bmatrix} R_{0,0} & \cdots & R_{0,nN_{code}-1} \\ & \ddots & \vdots \\ \mathbf{0} & & R_{nN_{code}-1,nN_{code}-1} \end{bmatrix} \begin{bmatrix} \bar{d}(0) \\ \vdots \\ \bar{d}(nN_{code} - 1) \end{bmatrix} + \mathbf{Q}^H \mathbf{N}. \quad (11)$$

From (11), the maximum likelihood sequence  $\hat{\mathbf{d}}_{ML}$  are given as

$$\hat{\mathbf{d}}_{ML} = \arg \min_{\bar{\mathbf{d}}} \left( \sum_{t=1}^{nN_{code}-1} \left| Z(nN_{code} - t) - \sqrt{2P} \sum_{t'=0}^t R_{nN_{code}-t, nN_{code}-t'} \bar{d}(nN_{code} - t') \right|^2 \right), \quad (12)$$

where  $\hat{\mathbf{d}} = [\hat{d}(0), \dots, \hat{d}(nN_{code} - 1)]^T$  is the symbol vector candidate.

Then, M algorithm is performed as follows [8,9]. At the  $t$ th ( $t=0, \dots, nN_{code}-1$ ) stage, after calculating the path metric using the squared Euclidian distance for a candidate sequence, the sum of path metric until the  $t$ th stage called as cumulative path metric is computed. Then, the best  $M$  candidate sequences are selected as surviving symbol candidates by comparing the cumulative path metrics. The above operations are repeated until the last stage. At the last stage, the data demodulation is carried out by choosing the symbol candidate sequence having the smallest cumulative path metric. The behavior of M algorithm is illustrated in Fig. 3.

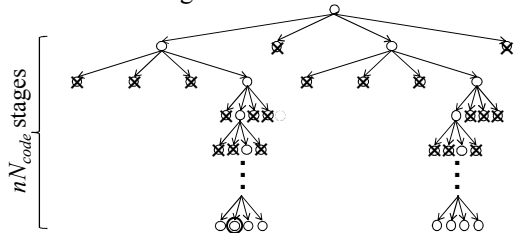


Fig. 3. Behavior of M algorithm (QPSK  $M=2$ ).

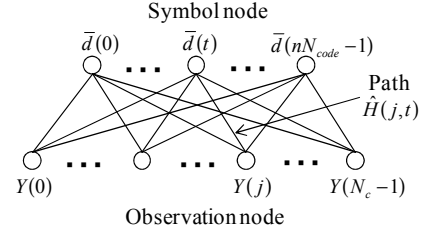


Fig. 4. Tanner graph expression.

### C. BP

In PBC-SC transmission, the concatenation of channel matrix, mapping matrix, DFT matrix, interleaving matrix and pseudo block encoding matrix can be viewed as an equivalent MIMO channel and hence, the received signal can be expressed by tanner graph shown in Fig. 4. Therefore, FDE, de-mapping, IDFT, de-interleaving and pseudo block decoding can be jointly performed by applying BP while reducing the computational complexity.

Below, we explain the behavior of BP focusing on the  $i$ th ( $i=0, \dots, I-1$ ) iteration.

#### (a) Operations at observation node

At the  $j$ th ( $j=0, \dots, N_c-1$ ) observation node, ISI cancellation is performed by using soft-decision symbol replicas, which are generated from extrinsic LLRs transmitted from the symbol nodes. The received signal,  $\tilde{R}^{(i)}(j,t)$ , after ISI cancellation can be expressed as

$$\tilde{Y}^{(i)}(j,t) = Y(j) - \sqrt{2P} \sum_{\substack{t'=0 \\ \neq t}}^{nN_{code}-1} \hat{H}(j,t') \hat{d}^{(i-1)}(j,t'), \quad (13)$$

where  $\hat{H}(j,t')$  is the element of the equivalent MIMO channel in the  $j$ th row and  $t'$ th column.  $\hat{d}^{(i-1)}(j,t')$  is the soft-decision symbol replica generated in the  $(i-1)$ th iteration. When using QPSK data modulation, it is given as

$$\hat{d}^{(i-1)}(j,t') = \frac{1}{\sqrt{2}} \left\{ \tanh\left(\frac{\beta^{(i-1)}(j,t',0)}{2}\right) + j \tanh\left(\frac{\beta^{(i-1)}(j,t',1)}{2}\right) \right\}, \quad (14)$$

where  $\beta^{(i-1)}(j,t',u)$  is the extrinsic LLR of the  $u$ th bit transmitted from the  $t'$ th symbol node. The  $j$ th observation node computes LLR,  $\alpha^{(i)}(j,t,u)$ , of the  $u$ th bit  $b(t,u)$  in the  $t$ th symbol from the received signal after ISI cancellation given as

$$\alpha^{(i)}(j,t,u) = \log \frac{\Pr(\tilde{Y}^{(i)}(j,t)|b(t,u)=1)}{\Pr(\tilde{Y}^{(i)}(j,t)|b(t,u)=0)}$$

$$\approx \frac{1}{2(\sigma^{(i)}(j,t))^2} \left( \left| \tilde{Y}^{(i)}(j,t) - \sqrt{2P} \hat{H}(j,t) d_{b(t,u)=0}^{\min} \right|^2 - \left| \tilde{Y}^{(i)}(j,t) - \sqrt{2P} \hat{H}(j,t) d_{b(t,u)=1}^{\min} \right|^2 \right), \quad (15)$$

where  $d_{b(t,u)=0}^{\min}$  (or  $d_{b(t,u)=1}^{\min}$ ) is the most probable symbol, which has the smallest Euclidian distance between the received signal, whose the  $m$ th bit is 0 (or 1).  $2(\sigma^{(i)}(j,t))^2$  is the variance of the residual ISI plus noise given as

$$2(\sigma^{(i)}(j,t))^2 = 2P \sum_{\substack{t'=0 \\ \neq t}}^{nN_{code}-1} |\hat{H}(j,t')|^2 \left( 1 - |\hat{d}^{(i-1)}(j,t')|^2 \right) + \frac{2N_0}{T_s}. \quad (16)$$

After performing the above operations at all observation nodes, LLRs  $\alpha^{(i)}(j,t,u)$  are transmitted to the symbol nodes.

### (b) Operations at symbol node

The  $t$ th ( $t=0, \dots, nN_{code}-1$ ) symbol node computes a posteriori LLR by adding all LLRs transmitted from the observation nodes. The posteriori LLR,  $\gamma^{(i)}(t, u)$ , of the  $u$ th bit in the  $t$ th symbol are given as

$$\gamma^{(i)}(t, u) = \sum_{j=0}^{N_c-1} \alpha^{(i)}(j, t, u). \quad (17)$$

Then, the symbol node computes the extrinsic LLR,  $\beta^{(i)}(j, t, u)$ , which is forwarded to the  $j$ th observation node given as

$$\beta^{(i)}(j, t, u) = \gamma^{(i)}(t, u) - \alpha^{(i)}(j, t, u). \quad (18)$$

After performing the above operation at all symbol nodes, the symbol nodes transmit it to the observation nodes.

The above LLR exchange between the observation nodes and the symbol nodes is repeated by  $I$  iterations and finally, data demodulation is carried out by using the posteriori LLR,  $\gamma^{(I-1)}(t, u)$ , at the symbol node.

## IV. COMPUTER SIMULATION

In this paper, we consider pseudo (7,4) hamming code [5] as an initial study. We consider QPSK data modulation and the number of pseudo block coded sequences  $N_{code}$  is set to  $N_{code} = \lfloor N_c/k \rfloor$  where  $\lfloor x \rfloor$  is the largest integer smaller than or equal to  $x$ . We use  $k \times N_{code}$  block interleaver. In this paper, we assume that  $kN_{code}$  frequency components of transmit signal are consecutively mapped to  $N_c$  subcarriers as an initial study. Therefore, mapping matrix  $\mathbf{M}$  is given as  $\mathbf{M} = \text{diag}\{1, \dots, 1, 0, \dots, 0\}$ . FFT block size and CP length is set to  $N_c=64$  and  $N_g=16$ , respectively. The channel is assumed to be a frequency-selective block Rayleigh fading channel having symbol spaced  $L = 16$  path uniform power delay profile. We assume that channel estimation can be perfectly performed at the receiver.

### A. Impact of the number of iterations and surviving paths

Fig. 5 plots the BER performance when using PBC-SC transmission with FDBD aided FDED as the number of iterations and surviving paths parameter. It is seen from Fig. 5 that  $I=3$ ,  $M=8$  and  $I=5$  are sufficient to improve the BER performance when using FDIC, QRM-MLBD, and BP, respectively. Note that the sufficient number of surviving paths for QRM-MLBD in PBC-SC transmission is smaller than that in uncoded SC transmission [9]. The reason for this is explained as follows. In the case of uncoded SC transmission, the amplitude of an element of the upper triangle matrix  $\mathbf{R}$  closer to right positions may drops. Therefore, the probability of removing the correct symbol candidates at early stages increases if the number of surviving paths is small. To sufficiently improve the BER performance, the large number of surviving paths is required, resulting in large computational complexity [9]. On the other hand, in PBC-SC transmission, diversity gain can be obtained by pseudo block encoding and hence, the probability of removing the correct symbol candidates can be reduced. As a consequence, the sufficient BER performance improvement can be obtained even if the number of surviving paths is small.

### B. Comparison to MMSE based FDED and MF bound

Fig. 6 plots the BER performance of PBC-SC transmission with FDBD aided FDED as a function of the received  $E_b/N_0$ .

The number  $I$  of iterations and the number  $M$  of surviving paths are set to  $I=3$ ,  $M=8$  and  $I=5$  when using FDIC, QRM-MLBD and BP, respectively. For the comparison, the BER performances using MMSE based FDED and block coded SC transmission with 2-step decoding (which performs FDE and hard decision decoding separately) and MF bound are also plotted in Fig. 6. It is seen from Fig. 6 that PBC-SC transmission can achieve better BER performance than block coded SC transmission with 2-step decoding. This is because large frequency-diversity gain can be obtained by jointly performing FDE and pseudo block decoding. Also seen from Fig. 6 is that FDBD aided FDED can further improve BER performance compared to MMSE based FDED. For example, when the required BER is  $10^{-4}$ , FDIC, QRM-MLBD and BP can reduce the required  $E_b/N_0$  by 2.6dB, 3.0dB and 2.6dB, respectively, compared to MMSE based FDED. This is because FDBD aided FDED can mitigate the impact of ISI more than MMSE based FDED. It is also seen from Fig. 6 that the required  $E_b/N_0$  gap between FDBD aided FDED and MF bound is smaller than 0.4dB and all FDBD aided FDED schemes can achieve almost the same BER performance as MF bound.

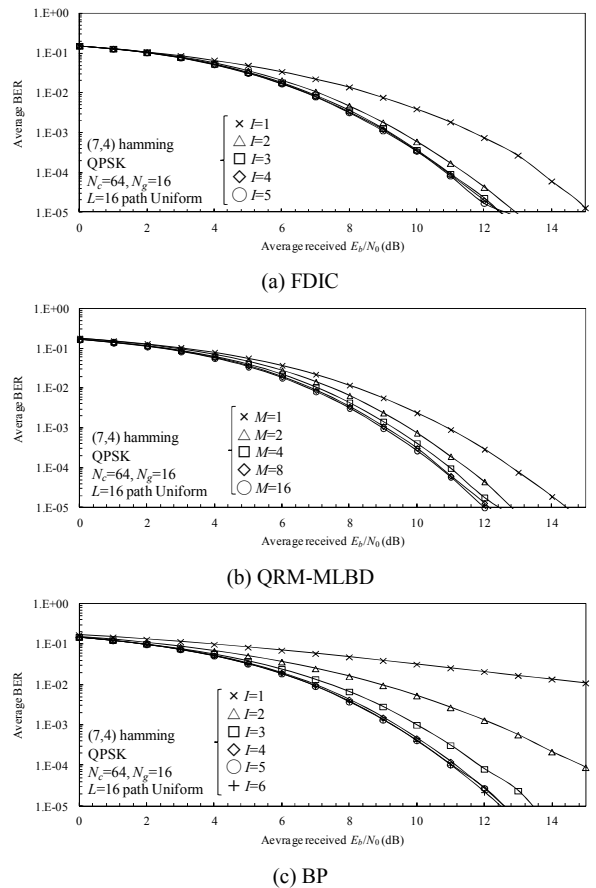


Fig. 5. BER performances with FDBD aided FDED.

### C. Computational complexity

The computational complexity when using each decoding scheme at the receiver is summarized in Table I. The computational complexity is defined as the number of real multiplications per block.  $X$  denotes the number of bits per block and  $Z$  is the largest integer which satisfies  $X^Z < M$ . FDIC requires

MMSE filtering and iterative operation and hence, the computational complexity of FDIC is proportional to  $I(N_c)^3$ . On the other hand, PBC-SC transmission can reduce the required number of surviving paths for M algorithm and hence, the computational complexity of QRM-MLBD depends on QR decomposition. Therefore, the computational complexity of QRM-MLBD is proportional to  $N_c(nN_{code})^2$  and is almost the same order as that of MMSE based FDED. BP requires equivalent channel matrix computation, ISI cancellation and LLR computation. Therefore, the computational complexity of BP is proportional to  $lnk(N_{code})^2$ . Fig. 7 plots the computational complexity normalized by that of 2-step decoding as a function of the required  $E_b/N_0$  for BER= $10^{-5}$ . It is seen from Fig. 7 that QRM-MLBD can achieve almost the same required  $E_b/N_0$  as MF bound with 2 times lower computational complexity than MMSE based FDED. This is because PBC-SC transmission can reduce the required number of surviving paths for M algorithm due to large frequency-diversity gain. It is also seen from Fig. 7 that BP can achieve about 0.4dB  $E_b/N_0$  degradation from MF bound while requiring 8 times lower computational complexity compared to MMSE based FDED.

### V. CONCLUSION

In this paper, we proposed FDBD aided FDED for PBC-SC transmission in order to narrow the performance gap from MF bound. We presented three FDBD aided FDED schemes: FDIC, QRM-MLBD and BP. It was shown by computer simulation that PBC-SC transmission can reduce the number of surviving paths for M algorithm and as a consequence, QRM-MLBD requires 2 times lower computational complexity than MMSE based FDED while achieving the BER performance close to MF bound. It was also shown that BP achieves almost the same BER performance as MF bound while requiring about 8 times lower computational complexity than MMSE based FDED. In this paper, as an initial study we considered a simple pseudo (7,4) hamming code. Application of more complex block code, such as LDPC code, to PBC-SC transmission with FDBD aided FDED is left as our future work.

### REFERENCES

- [1] J. G. Proakis and M. Salehi, Digital communications, 5th edition, McGraw-Hill, 2008.
- [2] H. Sari, G. Karam, and I. Jeanclaude, "Transmission technique for digital terrestrial TV broadcasting," IEEE Commun. Mag., vol. 33, no. 2, pp. 100-109, Feb. 1995.
- [3] D. Falconer, S. L. Ariyavistakul, A. Benyamin-Seeyar, and B. Edison, "Frequency domain equalization for single-carrier broadband wireless systems," IEEE Commun. Mag., vol. 40, no. 4, pp. 58-66, Apr. 2002.
- [4] F. Adachi, H. Tomeba, and K. Takeda, "Introduction of frequency-domain signal processing to broadband single-carrier transmission in a wireless channel," IEICE Trans. Commun., vol. E92-B, pp. 2789-2808, Sept. 2009.
- [5] H. Miyazaki and F. Adachi, "Pseudo Block Coded Single-Carrier Frequency-Domain Equalization Transmission," Proc. 2014 IEEE 80th Vehicular Technology Conference (VTC2014fall), Vancouver, Canada, Sept. 2014.
- [6] A. Nakajima and F. Adachi, "iterative FDIC using 2D-MMSE-FDE for turbo-coded HARQ in SC-MIMO multiplexing," IEICE Trans. Commun., vol. E90-B, no. 3, pp. 693-695, Mar. 2007.
- [7] S. Okuyama, K. Takeda and F. Adachi, "Iterative MMSE detection and interference cancellation for uplink SC-FDMA MIMO using HARQ," Proc. IEEE International Conference on Communication, June 2011.
- [8] K. Nagatomi, K. Higuchi and H. Kawai, "Complexity reduced MLD based on QR decomposition in OFDM MIMO multiplexing with

frequenc-domain spreading and code multiplexing," Proc. IEEE Wireless Communications and Networking Conference (WPNC2009), pp. 1-6, Apr. 2009.

- [9] T. Yamamoto, K. Takeda and F. Adachi, "Single-carrier transmission using QRM-MLD with antenna diversity," Proc. 12th International Symposium on Wireless Personal Multimedia Communications (WPMC2009), Sept. 2009.
- [10] W. Fukuda, T. Abiko, T. Nishimura, T. Ohgane, Y. Ogawa, Y. Ohwatari and Y. Kishiyama, "Low-complexity detection based on belief propagation in a massive MIMO system," Proc. 2013 IEEE 77th Vehicular Technology Conference (VTC2013spring), pp. 1-5, June 2013.
- [11] W. Fukuda, T. Abiko, T. Nishimura, T. Ohgane, Y. Ogawa, Y. Ohwatari and Y. Kishiyama, "Complexity reduction for signal detection based on belief propagation in a massive MIMO system," Proc. 2013 International Symposium on Intelligent Signal Processing and Communications Systems (ISPACS2013) pp. 245-250, Nov. 2013.

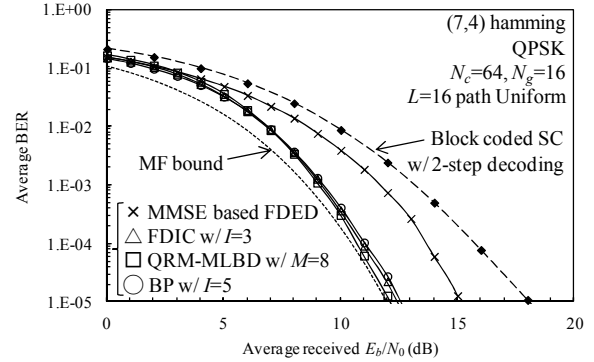


Fig. 6. Comparison to MMSE based FDED and MF bound.

TABLE I. COMPUTATIONAL COMPLEXITY

2-step decoding		MMSE filtering		FDIC	
FFT	$5N_c \log_2 N_c$	FFT	$5N_c \log_2 N_c$	FFT	$5N_c \log_2 N_c$
FDE weight computation	$4N_c$	Equivalent channel matrix computation	$7nk(N_{code})^2 + 2nkN_{code}$	Equivalent channel matrix computation	$7lnk(N_{code})^2 + 2lnkN_{code}$
FDE	$4N_c$				
De-mapping	$2N_c$	MMSE weight computation	$4n^2k(N_{code})^3 + 4(nN_{code})^3 + 4n^2k(N_{code})^3$	MMSE weight computation	$2lnk(N_{code})^2 + 4l(nN_{code})^2 + 4l(N_c)^3 + 4ln_c(nN_{code})^2$
IDFT	$4(kN_{code})^2$	MMSE filtering	$4nN_{code}N_c$	MMSE filtering	$4lnN_{code}N_c$
De-interleaving	$2kN_{code}$			Replica generation	$4lnk(N_{code})^3 + 4lnN_{code} \times (nN_{code}+1)$
Block decoding	$12N_{code}$				
QRM-MLBD		Belief Propagation			
FFT	$5N_c \log_2 N_c$	FFT	$5N_c \log_2 N_c$		
Equivalent channel matrix computation	$7nk(N_{code})^2 + 2nkN_{code}$	Equivalent channel matrix computation	$7lnk(N_{code})^2 + 2lnkN_{code}$		
QR decomposition	$4N_c(nN_{code})^2 + 4nN_{code}N_c$	Interference cancellation	$4ln_c(nN_{code}-1)$		
Metric computation	$\frac{4nXN_{code}^2}{4(X-Z+1)^{c+1}} + \frac{2Z^2(X-Z-1)}{2M(nN_{code}-Z)} \times (nN_{code}-Z) + 2X(Z+1)(X-1) + 2MX(nN_{code}-Z)$	LLR computation	$4lnN_cN_{code}$		

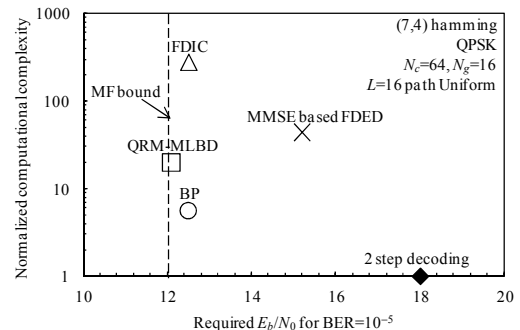


Fig. 7. Required  $E_b/N_0$  v.s. normalized computational complexity.